

Breakdown of order-fractionalization in the CPT model

Aaditya Panigrahi,¹ Alexei Tsvelik,² and Piers Coleman^{1,3}

¹*Center for Materials Theory, Department of Physics and Astronomy, Rutgers University, 136 Frelinghuysen Rd., Piscataway, NJ 08854-8019, USA*

²*Division of Condensed Matter Physics and Materials Science, Brookhaven National Laboratory, Upton, NY 11973-5000, USA*

³*Department of Physics, Royal Holloway, University of London, Egham, Surrey TW20 0EX, UK.*

(Dated: July 15, 2024)

We present an analysis of the half-filled CPT model, an analytically tractable Kondo lattice model with Yao-Lee spin-spin interactions on a 3D hyperoctagon lattice, proposed by Coleman, Panigrahi, and Tsvelik. Previous studies have established that the CPT model exhibits odd-frequency triplet superconductivity and order fractionalization. Through asymptotic analyses in the small J and large J Kondo coupling limits, we identify a quantum critical point at J_c , marking a transition from a superconductor to a Kondo insulator. By estimating the vison gap energy to account for thermal gauge fluctuations, we determine the energy scales governing the thermal breakdown of order fractionalization. Moreover, at large J the Kondo insulator undergoes orbital decoupling, leading to the formation of a decoupled Kitaev orbital liquid. These findings and analogies with the \mathbb{Z}_2 -gauged XY model lead us to propose a tentative phase diagram for the CPT model at half-filling.

I. INTRODUCTION

In heavy fermion materials, the coherent scattering of conduction electrons off a lattice of local moments produces a wide variety of emergent behavior. These range from heavy fermion metals and superconductors [1–6] to topological Kondo Insulators [7, 8]. Broader classes of flat band systems, such as Moiré materials can also be modeled as heavy fermion systems[9–11].

An insightful approach to heavy fermions is to consider them as the Higgs phase[12–16] of an underlying spin-liquid. From this perspective, alternate patterns of spin fractionalization may drive new kinds of physics, such as pairing beyond the BCS paradigm. One way to explore this idea is to study Kondo lattices with a pre-formed spin liquid. Attempts have focused on understanding Kondo lattice models, where the underlying spins interact via Kitaev interactions[5, 6, 17]. Unfortunately, Kitaev-Kondo models lose their exact solvability as a result of the Kondo term: to avoid this difficulty, Coleman, Panigrahi, and Tsvelik (CPT) have recently proposed a three-dimensional Kondo lattice model, [3, 4](Fig. 1) in which a Yao-Lee orbital-spin interaction[18] restores the solvability of the Kondo lattice at half filling.

The Hamiltonian for the CPT model on a hyperoctagon lattice (Fig 1),

$$H_{CPT} = H_c + H_{YL} + H_K \quad (1)$$

has three components:

$$H_c = -t \sum_{\langle i,j \rangle} (c_{i\sigma}^\dagger c_{j\sigma} + \text{H.c.}) - \mu \sum_i c_{i\sigma}^\dagger c_{i\sigma}, \quad (2)$$

$$H_{YL} = K/2 \sum_{\langle i,j \rangle} \lambda_i^{\alpha_{ij}} \lambda_j^{\alpha_{ij}} (\vec{S}_i \cdot \vec{S}_j), \quad (3)$$

$$H_K = J \sum_i (c_i^\dagger \vec{\sigma}_i) \cdot \vec{S}_i \quad (4)$$

Here $\langle i, j \rangle$ are neighboring sites on the hyper-octagonal lattice[19], a trivalent body centered cubic (BCC) crystal with four atoms per primitive unit cell, coiled around a helix to form alternating square and octagonal spirals(Fig. 1b). Each site supports both electrons $c_{i\sigma}$, localized spins \vec{S}_i and localized orbital $\vec{\lambda}_i$ degrees of freedom. The conduction term H_c describes electrons hop-

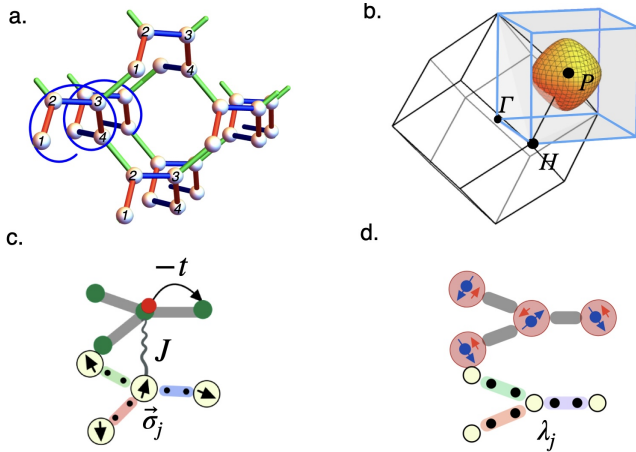


FIG. 1. (a) The hyperoctagon lattice, a trivalent structure consisting of a spiral of four atoms per unit cell embedded in a body centered cubic lattice. (b) A Yao-Lee spin liquid on this lattice results in a flux-free gauge configuration, giving rise to a Majorana Fermi surface centered at the $P = (\pi, \pi, \pi)$ point in the Brillouin zone. (c) Schematic showing the Kondo coupling between the conduction electrons and the local moments. (d) Cartoon illustrating the ground-state of the large J region of the CPT model, showing in pink, the formation of Kondo singlets between conduction electrons and spins and a decoupled Kitaev orbital liquid (KOL) .

ping between nearest neighboring sites. The Kondo interaction H_K antiferromagnetically couples the conduction electrons to spins \vec{S}_i at each site. Finally, the Yao-Lee term couples the orbitals $\vec{\lambda}_i$ via a Kitaev-like anisotropic interaction, “decorated” by a Heisenberg coupling between the nearest neighbor spins \vec{S}_i . The α_{ij} are the Ising coupling of orbital components along the $\alpha_{ij} = x, y, z$ bond directions (Fig. 1c).

The anisotropic Ising coupling between orbitals induces Majorana fractionalization [18] of spins $\vec{S}_j = -(\frac{i}{2})\vec{\chi}_j \times \vec{\chi}_j$ and orbitals $\vec{\lambda}_i = i\vec{b}_j \times \vec{b}_j$. In the physical Hilbert space, where $\sigma_j^a \lambda_j^\alpha = 2i\chi_j^a b_j^\alpha$, the fractionalized form of the Yao-Lee Hamiltonian H_{YL} (3) is

$$H_{YL} = K \sum_{\langle i,j \rangle} \hat{u}_{ij} (i\vec{\chi}_i \cdot \vec{\chi}_j). \quad (5)$$

Here, $\hat{u}_{ij} = ib_i^{\alpha ij} b_j^{\alpha ij}$ are the static \mathbb{Z}_2 gauge fields, (i.e. $[H_{YL}, \hat{u}_{ij}] = 0$).

In three dimensions, \mathbb{Z}_2 gauge theories undergo a finite temperature Ising phase transition at T_{c1} , into a deconfined phase, in which the vortices (plaquettes with a π flux) are linearly confined. In the Yao Lee model on a hyper-octagonal lattice, $T_{c1} \sim 0.036K$ [4, 20, 21], leading to a fractionalization of the spins into majoranas at lower temperatures $T < T_{c1}$.

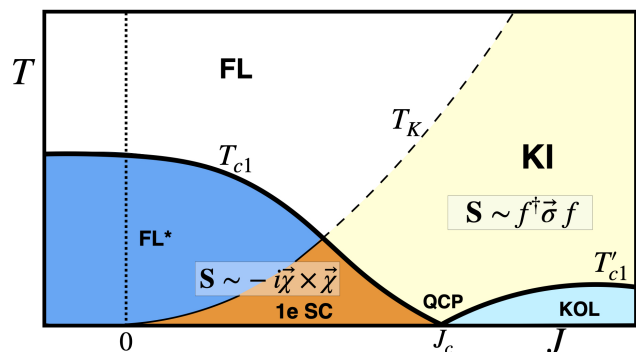


FIG. 2. Proposed phase diagram of the half-filled CPT model at half-filling. A finite temperature Fermi liquid (FL) with a small Fermi surface (FL) develops at small J , with a cross-over into a Kondo insulating phase KI at large J . For $T < T_{c1}$ and small J , the spins fractionalize into Majorana ($\vec{\chi}$) fermions, forming a 3D Yao Lee spin liquid. A logarithmic divergence in the pairing susceptibility at small positive J gives rise to a charge $1e$, $S = 1/2$ electron-majorana condensate (1eSC), with a transition temperature comparable to the single-ion Kondo temperature T_K . Once T_K exceeds T_{c1} , T_{c1} drops to zero at $J = J_c$, giving rise to a superconductor-insulator quantum critical point (QCP), forming a Kondo insulator (KI) where the spins fractionalize as Dirac (f) fermions. For $T < T'_{c1}$, the Kondo insulator co-exists with a decoupled Kitaev orbital-liquid (KOL).

In this paper, we examine the phase diagram (Fig. 2) of the CPT model at half-filling. Central to the phase diagram are the two characteristic energy scales: the

Kondo temperature T_K and the Ising transition temperature T_{c1} . Below the Kondo temperature ($T < T_K$) the conduction electrons screen the spins, while below the Ising temperature ($T < T_{c1}$) the spins fractionalize $\vec{S}_j = -\frac{i}{2}\vec{\chi}_j \times \vec{\chi}_j$ into $\vec{\chi}_j$ majoranas. The interplay between spin fractionalization and Kondo screening determines the phase diagram.

Our proposed phase diagram for the half-filled CPT model (CPTM), shown in Fig. 2, is based on the analytical tractability of the extreme limits of small and large J Kondo coupling, where the model exhibits superconductivity and Kondo insulating behavior, respectively. One or more quantum phase transitions at an intermediate coupling J_c must therefore separate these distinct phases.

Applying Ockham’s razor, we propose a single quantum critical point (QCP) defining the superconductor-insulator transition. While we cannot entirely rule out an alternative first-order quantum phase transition between the two phases, this scenario would necessitate a finite temperature critical endpoint, with a thermal rather than a quantum phase transition governing the changing pattern of spin fractionalization.

The Kondo temperature $T_K(J)$ and the Ising transition temperatures $T_{c1}(J)$ and $T'_{c1}(J)$ divide the phase diagram (Fig. 2) into five phases, which we summarize below:

1. *Fermi Liquid* (FL) ($5t \gg T > T_{c1}$ and $T > T_K$): At temperatures much higher than T_K and T_{c1} , but much lower than the conduction band-width $W \sim 5t$ the CPT model forms a conduction Fermi liquid, weakly coupled to its embedded spins and orbitals. The spins and orbitals will exhibit paramagnetic behavior characterized by Curie-Weiss susceptibility.
2. *Fermi Liquid** (FL*) ($T < T_{c1}$ and $T > T_K$): Below the Ising transition temperature ($T < T_{c1}$) the spins fractionalize into Majorana fermions $\vec{S}_j = -\frac{i}{2}\vec{\chi}_j \times \vec{\chi}_j$, forming a Yao-Lee spin liquid with a Majorana Fermi surface. Since the system is above the Kondo temperature ($T > T_K$), the Yao-Lee spin liquid remains unscreened by the conduction sea. Thus, in this phase, the CPT model consists of a decoupled Fermi liquid and a Yao Lee spin liquid, constituting a Fermi liquid* phase.
3. *1e Superconductor* (1e SC) ($T < T_{c1}$ and $T < T_K$): In this phase, spins undergo Majorana fractionalization and experience Kondo screening by conduction electrons. The precise nesting between the Majorana Fermi surface of the Yao-Lee spin liquid and the conduction sea at half-filling results in a Peierls-like logarithmic instability between the electron and Majorana Fermi surface for an infinitesimal Kondo coupling [4].

This results in an odd-frequency triplet superconductor characterized by a fractionalized charge e

spinor order in the small J -limit [3, 4, 22]. The system exhibits a neutral Fermi surface due to an imbalance between 4 conduction Majoranas and 3 spin liquid Majoranas. For more details see section II.

4. *Kondo Insulator* (KI) ($T_K > T > T_{c1}, T'_{c1}$) Below the Kondo temperature T_K , but at temperatures larger than the Ising temperatures T_{c1}, T'_{c1} , the spins are screened by the conduction sea, forming a Kondo insulator, while the decoupled orbitals are unfractioalized.
5. *Kitaev Orbital Liquid* (KOL) The ground state properties of the Kondo insulator at large J can be determined by carrying out a strong coupling expansion in $1/J$. In this limit, the ground-state is a product ground state of local Kondo singlets ($(\uparrow\downarrow - \downarrow\uparrow)_j$), co-existing with a degenerate manifold of decoupled orbitals λ_j^α

$$|\Psi\rangle = \prod_j (\uparrow\downarrow - \downarrow\uparrow)_j \{ \lambda_j \}. \quad (6)$$

The large spin-gap of order J in this phase allows a treatment of the Heisenberg bond operator $\vec{S}_i \cdot \vec{S}_j \sim \langle \vec{S}_i \cdot \vec{S}_j \rangle \sim O(t/J)$ as a static variable. Through the Yao-Lee coupling, this lifts the orbital degeneracy, giving rise to a decoupled 3D Kitaev orbital liquid (orbital analog of Kitaev spin liquid) below the second Ising transition temperature T'_{c1} . For more details see section III.

This paper is structured as follows: in section II we summarize the small- J limit of the CPT model; in section III we present the large- J limit, while in the final section IV we discuss the intermediate coupling behavior of the CPT model.

II. SMALL- J LIMIT OF THE CPT MODEL

For completeness, here we summarize the results of our previous work[4] on the half-filled CPT model in the analytically tractable small J limit.

We recall that the CPT model is a Kondo lattice model with a quartet state at each site, comprised of a $S = 1/2$ spin and orbital degree of freedom at each site. The Yao-Lee interaction between sites acts to establish an emergent static \mathbb{Z}_2 field[3, 4]. At half filling, the CPT model develops nested electron and Majorana Fermi surfaces and for infinitesimal Kondo coupling, the system undergoes a second-order phase transition into a spinor-ordered electron-majorana condensate[4].

Yao Lee spin-liquid: The three dimensional Yao Lee (3DYL) model on a hyperoctagon lattice shares many of the properties of a 2D Kitaev spin liquid, most notably, the presence of gapped \mathbb{Z}_2 flux excitations, described by Wilson loops - products of the gauge fields

$W = \prod u_{(i,j)} = \pm 1$ around closed ten-fold loops of the hyperoctagon lattice (where (i,j) orders the sites i and j along xx , yy and zz bonds so that the site furthest in the y , z and x directions respectively, is placed first [19]). In the spin liquid ground-state, all loops are trivial $W = 1$ [19]; flipping the sign of a Wilson loop creates a flux excitation (vison), with an energy determined as a fraction of K . Unlike 2D Kitaev spin liquids, the 3DYL undergoes an Ising phase transition at $T_{c1} \sim 0.036K$ into a Higgs phase where the elementary \mathbb{Z}_2 gauge excitations (visons) are linearly confined [4, 23–25]. and the Majorana fields describe coherent, fractionalized spin excitations.

Below the Ising transition temperature T_{c1} , the confinement of visons in the 3D Yao Lee model allows a gauge choice $u_{i,j} = 1$ [20] leading to a translationally invariant Hamiltonian. Transforming to a momentum basis,

$$\vec{\chi}_{\mathbf{k},\alpha} = \frac{1}{\sqrt{N}} \sum_j \vec{\chi}_{j\alpha} e^{-i\mathbf{k}\cdot\mathbf{R}_j}, \quad (7)$$

where \mathbf{R}_j is the position of the unit-cell in the BCC lattice, N is the number of primitive unit cells in the lattice and $\alpha \in [1, 4]$ is the site index within each unit cell. The ground state Hamiltonian for the Yao-Lee spin liquid is then

$$H_{YL} = K \sum_{\mathbf{k} \in \frac{\mathbb{BZ}}{2}} \vec{\chi}_{\mathbf{k},\alpha}^\dagger h(\mathbf{k})_{\alpha,\beta} \vec{\chi}_{\mathbf{k},\beta}, \quad (8)$$

where $\alpha, \beta \in [1, 4]$ are the site indices and

$$h(\mathbf{k}) = \begin{pmatrix} 0 & i & ie^{-i\mathbf{k}\cdot\mathbf{a}_2} & ie^{-i\mathbf{k}\cdot\mathbf{a}_1} \\ -i & 0 & -i & ie^{-i\mathbf{k}\cdot\mathbf{a}_3} \\ -ie^{i\mathbf{k}\cdot\mathbf{a}_3} & i & 0 & -i \\ -ie^{i\mathbf{k}\cdot\mathbf{a}_1} & -ie^{i\mathbf{k}\cdot\mathbf{a}_2} & i & 0 \end{pmatrix} \quad (9)$$

where $\mathbf{a}_1 = (1, 0, 0)$; $\mathbf{a}_2 = \frac{1}{2}(1, 1, -1)$; $\mathbf{a}_3 = \frac{1}{2}(1, 1, 1)$, are the primitive BCC lattice vectors. Since $\chi_{-\mathbf{k}} = \chi_{\mathbf{k}}^\dagger$, the momentum sum is restricted to half the Brillouin zone, corresponding to a cube ($\frac{\mathbb{BZ}}{2}$) of side length 2π centered at the P point at (π, π, π) . The spectrum $E_{\mathbf{k}} \equiv K\epsilon(\mathbf{k})$, determined by $\det[\epsilon\mathbb{1} - h(\mathbf{k})] = 0$, or

$$\epsilon^4 - 6\epsilon^2 - 8\epsilon(s_x s_y s_z) + [9 - 4(s_x^2 + s_y^2 + s_z^2)] = 0, \quad (10)$$

(where $s_l \equiv \sin(k_l/2)$, $l = x, y, z$), contains a *single* Fermi surface where $\epsilon = 0$ and $s_x^2 + s_y^2 + s_z^2 = 9/4$, centered at P [26]. (Fig. 1 b.)

Conduction electrons: The nesting between Majorana and conduction Fermi surface becomes evident upon performing the gauge transformation $(c_1, c_2, c_3, c_4)_{\vec{R}} \rightarrow e^{i(\pi, \pi, \pi)\cdot\mathbf{R}}(c_1, ic_2, c_3, -ic_4)_{\vec{R}}$ on conduction electrons in the unit-cell at \vec{R} . The resulting conduction Hamiltonian H_c takes the form,

$$H_c = \sum_{\mathbf{k} \in \mathbf{BZ}} c_{\mathbf{k},\sigma\alpha}^\dagger [-t h(\mathbf{k}) - \mu\mathbb{I}]_{\alpha\beta} c_{\mathbf{k},\sigma\beta}, \quad (11)$$

where α, β denote the site indices of the unit cell, thus sharing the same hopping matrix $h(\mathbf{k})$ (8) as the spinons

in the 3D Yao Lee spin liquid. At $\mu = 0$, the conduction sea develops an electron and a hole Fermi surface at P and $-P$ respectively, which can be rewritten as four Majorana Fermi surfaces centered at P . These Fermi surfaces perfectly nest with the three Majorana Fermi surface of the spin liquid, which facilitates a BCS-like mean-field treatment of the Kondo interaction.

Kondo interaction: To this end, we express the Kondo interaction in Majorana spin representation as,

$$H_K = J \sum_j (c_j^\dagger \vec{\sigma} c_j) \cdot \left(-\frac{i}{2} \vec{\chi}_j \times \vec{\chi}_j\right) \equiv -\frac{J}{2} \sum_l c_j^\dagger (\vec{\chi} \cdot \vec{\sigma})^2 c_j \quad (12)$$

Small- J limit: Below the Ising transition T_{c1} a Hubbard-Stratonovich transformation of the Kondo interaction in terms of the charge- e spinor order $V_j = -J \langle \vec{\chi}_a \cdot \vec{\sigma} c_j \rangle = (V_{j\uparrow}, V_{j\downarrow})^T$,

$$H_K = \sum_j [c_j^\dagger (\vec{\sigma} \cdot \vec{\chi}_j) V_j + \text{H.c.}] + \frac{2V_j^\dagger V_j}{J}. \quad (13)$$

The uniform saddle point of the Hamiltonian then provides us with the mean-field solution[3, 4] in the small J limit. The mismatch in the number of conduction (4) and spin liquid majoranas (3) in equation (13) results in one conduction majorana remaining gapless as the fractionalized order condenses.

In the mean-field solution with uniform spinor configuration $V_{j\sigma} = (V/\sqrt{2})z_\sigma$, the electronic self-energy in momentum space is expressed as:

$$\Sigma_{\mathbf{k},\omega} = (1 - \mathcal{Z} \otimes \mathcal{Z}^\dagger) V^2 D(\mathbf{k}, \omega) \quad (14)$$

where $\mathcal{Z} = [z, i\sigma_y z^*]^T$ is the spinor order in Balian-Werthamer notation, and $D(\mathbf{k}, \omega) = [\omega - Kh(\mathbf{k})]^{-1}$ is the spin-liquid propagator. The matrix $\mathcal{Z} \otimes \mathcal{Z}^\dagger$ projects out one Majorana component of the conduction sea, leaving three components of the conduction sea to hybridize with the spin-liquid, gapping them out in a fashion similar to a Kondo insulator. The component of the conduction sea projected onto the spinor \mathcal{Z} forms a gapless ‘‘neutral’’ Fermi surface.

The superconducting nature of the spinor order phase is evident when expressing the self-energy in terms of three orthogonal d-vectors, formed from bilinears of the spinors, [4]:

$$\hat{\mathbf{d}}^1 + i\hat{\mathbf{d}}^2 = z^T (-i\sigma_2) \sigma z, \quad \hat{\mathbf{d}}^3 = z^\dagger \sigma z. \quad (15)$$

Written in terms of the d-vectors, the self-energy separates into magnetic and pairing components:

$$\Sigma = \Sigma_N(\mathbf{k}, \omega) + \Delta(\mathbf{k}, \omega) \tau_+ + \Delta^\dagger(\mathbf{k}, \omega) \tau_-, \quad (16)$$

which describe the coexistence of odd-frequency magnetism and triplet superconducting order, where

$$\Sigma_N(\mathbf{k}, \omega) = \frac{1}{4} (3 - (\hat{\mathbf{d}}^3 \cdot \sigma) \tau_3) \Sigma_0(\mathbf{k}, \omega)$$

describes odd-frequency magnetism and

$$\Delta(\mathbf{k}, \omega) = -\frac{1}{4} [(\hat{\mathbf{d}}^1 + i\hat{\mathbf{d}}^2) \cdot \sigma] \Sigma_0(\mathbf{k}, \omega),$$

describes the triplet superconductivity. Here

$$\Sigma_0(\mathbf{k}, \omega) = V^2 D(\mathbf{k}, \omega) \quad (17)$$

describes the hybridization with the spin liquid. On the Fermi surface of the spin liquid, $\Sigma_0(\mathbf{k}_F, \omega) \sim \frac{1}{\omega}$ is an odd function of frequency. The complex d-vector $\hat{\mathbf{d}}^1 + i\hat{\mathbf{d}}^2$ breaks the time-reversal symmetry, representing the two component superconducting order in the small- J limit.

The exactness of the small- J limit is a consequence of a logarithmic divergence in the pairing susceptibility, which results in a second-order phase transition at a transition temperature (Fig. 2),

$$T_K = W \exp\left(-\frac{1 + K/t}{\rho J}\right). \quad (18)$$

At temperatures $T < T_K$, the system forms an electron-majorana pair condensate with a spinor order parameter. Here, small J , combined with the logarithmic divergence of the spinor pair susceptibility, acts as the small parameter for the mean-field theory. Further, this spinor order generates odd-frequency triplet pairing within the conduction sea.

III. LARGE J LIMIT OF THE CPT MODEL

The large J limit of the half-filled CPT model can be solved in a strong coupling expansion in $1/J$. In this limit the half-filled ground state is a product state of local singlets of electrons and spins at each site (Fig. 1d), forming a Kondo insulator i.e.,

$$|\Psi\rangle = \prod_j (\uparrow\downarrow - \downarrow\uparrow)_j |\{\lambda_j\}\rangle. \quad (19)$$

where the ket $|\{\lambda_j\}\rangle$ describes an arbitrary configuration of the orbital degrees of freedom. There is a gap $\Delta_g = J$ between the singlet ground-state and the triplet excited states which allows us to carry out a strong coupling expansion in powers of K/J and t/J .

To first order in the expansion, $\langle \vec{S}_i \cdot \vec{S}_j \rangle = 0$ and the expectation value of the Yao Lee term (3) is zero. However, electron hopping (Fig. 3) gives rise to first-order corrections to the ground state:

$$|\Psi\rangle = |\Psi_0\rangle + \sum_j \frac{|j\rangle \langle j| \hat{H}_c |\Psi_0\rangle}{E_0 - E_j}, \quad (20)$$

where,

$$\hat{H}_c = -it \sum_{\langle i,j \rangle} (c_{i\sigma}^\dagger c_{j\sigma} - \text{H.c.}) \quad (21)$$

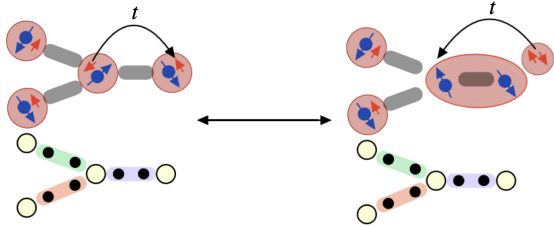


FIG. 3. Depicts the Kondo insulator phase of the CPT model. The ground state is a product state of local electron-local spin singlets, resulting in decoupled orbitals. Through the virtual hopping of conduction electrons between nearest neighbors, the Kondo singlet breaks into nearest neighbor holon-doublon virtual excitation, and the spins form a singlet. The system reverts to its original state via back-hopping to form a product state of Kondo singlets. This virtual excitation leads to the orbitals fractionalizing into Majorana, resulting in a decoupled Kitaev orbital liquid.

Written out explicitly,

$$|\Psi\{\lambda_j\}\rangle = \left(1 - \frac{2}{3J} \left[-it \sum_{\langle i,j \rangle} (c_{i\sigma}^\dagger c_{j\sigma} - H.c.) \right] \right) |\Psi_0\{\lambda_j\}\rangle. \quad (22)$$

The hopping moves one electron to a neighboring site forming a doubly occupied singlet state, leading to two unscreened local moments \vec{S}_i and \vec{S}_j . Since the hopping preserves the spin-singlet character of the wavefunction, the two unscreened neighboring spins must form a singlet with $\vec{S}_i \cdot \vec{S}_j = -\frac{3}{4}$. Thus to leading order

$$\langle \Psi\{\lambda_j\} | \vec{S}_i \cdot \vec{S}_j | \Psi\{\lambda_j\} \rangle = 2 \times \left(-\frac{3}{4}\right) \times \left(\frac{2t}{3J}\right)^2 = -\frac{2}{3} \frac{t^2}{J^2}. \quad (23)$$

In the low energy degenerate manifold of orbital states, the matrix elements of the Yao-Lee interaction are

$$\begin{aligned} \langle \Psi\{\lambda_j\} | H_{YL} | \Psi\{\lambda_j\} \rangle &= \frac{K}{2} \sum_{\langle i,j \rangle} \langle \vec{\sigma}_i \cdot \vec{\sigma}_j \rangle \lambda_i^{\alpha_{ij}} \lambda_j^{\alpha_{ij}} \\ &= \frac{K^*}{2} \sum_{\langle i,j \rangle} \lambda_i^{\alpha_{ij}} \lambda_j^{\alpha_{ij}}, \end{aligned} \quad (24)$$

with a renormalized coupling

$$K^* = -\frac{8}{3} \frac{t^2}{J^2} K. \quad (25)$$

It follows that in the large Kondo coupling J limit, the ground state of the CPT model at half-filling is a product state of spin-singlets with a decoupled Kitaev orbital liquid.

IV. DISCUSSION

We now discuss the nature of the phase diagram at intermediate coupling. At small J , the localized spins fractionalizes into vector ($S = 1$) majoranas, $\vec{S}_j = -\frac{i}{2} \vec{\chi}_j \times \vec{\chi}_j$, while at large J , they fractionalize as Dirac fermions $\vec{S} = f_j^\dagger \vec{\sigma} f_j$. As the ground-state evolves from a small J superconductor to a large J Kondo insulator, we anticipate a superconductor-insulator transition. For reasons discussed below, we expect this transition to be continuous providing a new example of a deconfined quantum critical point, involving a transition from a \mathbb{Z}_2 Higgs 1e superconductor to a \mathbb{Z}_2 deconfined Kitaev orbital liquid.

There are a number of motivating arguments for a quantum-critical superconducting-insulator transition. Firstly, the transition involves a Fermi-surface transformation, from a conduction neutral Majorana Fermi surface in the superconductor to a Majorana Fermi surface of orbital excitations: this is reminiscent of the continuous transitions from a small to a large Fermi surface thought to occur in heavy fermion criticality[27–29]. Secondly, energetic arguments tell us that a transition from superconductor to orbital Kondo insulator will occur when magnetic energy of the spin liquid ($E_{mag} \sim -K$) drops below the Kondo energy gain ($E_{Kondo} \sim \frac{V^2}{W}$), resulting from the partial gapping of the conduction Fermi surface, where W is the band-width of the electrons. The critical value of $K_c \sim \frac{V^2}{W}$ where this takes place implies $T_K \gg K$, leading to a small vison gap energy ($\Delta_v \sim \frac{K^3}{V^2}$, (see Appendix A). This suggests a continuous zero-temperature phase transition via the collapse of the vison gap at the quantum critical point.

While the vison gap energy, $\Delta_v \sim T_{c1} \sim \frac{1}{J^2}$ [25] (Fig.

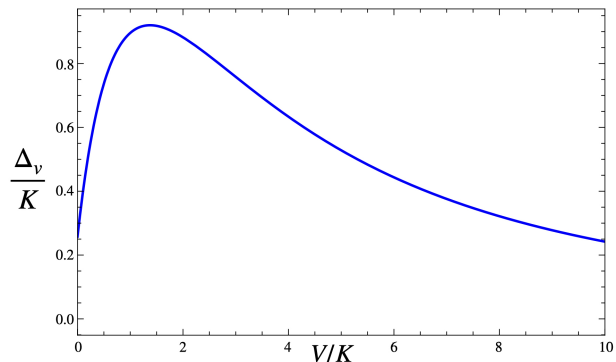


FIG. 4. (a) The vison gap Δ_v associated with a single bond flip $\hat{u}_{ij} = 1 \rightarrow -1$. Δ_v , is the characteristic energy scale of \mathbb{Z}_2 gauge fluctuations in the CPT model. The figure shows the vison gap as a function of the Kondo hybridization, calculated in the mean-field theory of the CPT model: this scale forms the boundary of the Ising phase transition T_{c1} in the regime $T_K > T_{c1}$. For large J , the hybridization $V \sim J$, so the large J behavior of vison gap energy allows us to estimate the Ising temperature as a function of Kondo coupling $\Delta_v \sim T_{c1} \sim \frac{1}{J^2}$.

4) representing the mass gap of the \mathbb{Z}_2 gauge theory, remains finite at all J in mean-field calculations (Appendix A), there is good reason to believe that quantum fluctuations will suppress this gap to zero at a finite J , producing a continuous superconducting-insulator transition. We expect that the zero point energy of spin-wave fluctuations, $E_{Qfl} \sim J^\alpha$ is a monotonically increasing function of J (i.e. $\alpha > 0$). The spin-liquid will remain energetically stable against gauge fluctuations provided $E_{Qfl} < \Delta_v$. As J increases, $E_{Qfl} \sim J^\alpha$ rises, while $\Delta_v \sim 1/J^2$ falls continuously, so we expect that this inequality fails at a finite critical J_c . Beyond this point, mean-field theory breaks down due to gauge fluctuations, and the system will transition into a Kondo insulator with a decoupled Kitaev orbital liquid.

In addition to the spin-wave fluctuations, \mathbb{Z}_2 gauge fluctuations will also tend to suppress the stability of the $1e$ superconductor. From our calculations of the energy spectrum associated with a single \mathbb{Z}_2 bond flip (Appendix A: Fig. 7), we observe the associated generation of spin $S = 1$ resonant Majorana modes within the spin liquid. When the superconducting gap V exceeds these resonant energies, they sharpen into long-lived bound-states. The concentration of these unscreened moments associated with bond-flips will follow an activated temperature dependence, $N \sim \exp(-\frac{(E_{bound} + \Delta_v)}{T})$, where E_{bound} is the Majorana bound-state energy. The appearance of unscreened triplet states implies a weakening of the Kondo screening associated with \mathbb{Z}_2 bond-flips in the superconducting phase, ultimately making the Kondo insulator, with its robust screening, more energetically favorable.

For these reasons, we believe that the Ising phase boundaries of the $1e$ superconductor and the Kitaev orbital liquid will merge at a quantum multicritical point. However, to definitively establish the nature of this quantum critical point requires further numerical investigation of the model using Monte Carlo and DMRG (on a lower dimensional analog), etc.

We now discuss the nature of the $1e$ superconducting phase and its finite temperature superconducting phase boundary. The $1e$ superconductor is a \mathbb{Z}_2 Higgs phase, and to understand its broken symmetry and its finite temperature phase diagram, we must go beyond mean-field theory. The mean-field spinor order parameter

$$V(x_j) = \langle (\vec{\sigma} \cdot \vec{\chi}_j) c_j \rangle \quad (26)$$

carries a \mathbb{Z}_2 gauge charge, and Elitzur's theorem guarantees that this quantity will average to zero under the thermal \mathbb{Z}_2 gauge fluctuations. However, this does not rule out the development of charge $2e$ composite triplet order associated with

$$\vec{\Psi}_{2e} = \langle V^T(x) i\sigma_2 \vec{\sigma} V(x) \rangle \quad (27)$$

which is \mathbb{Z}_2 gauge invariant, nor does it rule out the possibility of gauged off-diagonal long-range order, in which the charge $1e$ spinor order parameters at sites j

and i are linked by a product of gauge fields between the two sites,

$$\langle \hat{V}^\dagger(x) \hat{\mathcal{P}}(x,y) \hat{V}(y) \rangle \xrightarrow{|x-y| \rightarrow \infty} V^\dagger(x) V(y) \quad (28)$$

where $\hat{\mathcal{P}}(x,y) = \prod_l u_{(l+1,l)}$ along a path from y to x .

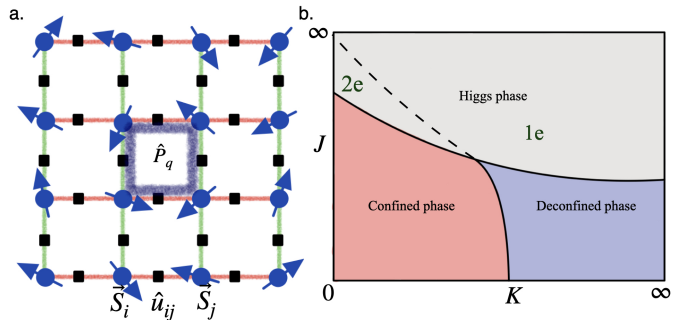


FIG. 5. (a) Depicts a \mathbb{Z}_2 gauge XY model where the XY spin interactions are gauged by \mathbb{Z}_2 bond variables \hat{u}_{ij} . Additionally, each plaquette P_q is formed by the product of \hat{u}_{ij} around the square, costs an energy K when going from $P_q = 1$ to $P_q = -1$. (b) Shows the phase diagram of \mathbb{Z}_2 gauged XY model in 3D cubic lattice. The model has 3 phases, 1. *Higgs phase*: In the Higgs phase, the spin \vec{S} gains long range order and vacuum expectation value. The dashed line represents the speculated phase boundary between the long-range ordered $e^{i\theta}$ and $e^{2i\theta}$ Higgs phases. 2. *Confined phase*: The confined phase is marked by the presence of deconfined $P_q = -1$, π -flux plaquettes spread through the ground state. 3. *Deconfined phase*: In this phase, π flux plaquettes are absent and \vec{S}_i s aren't long range ordered.

These two possibilities can be explored further by integrating out the fermions and then expanding the effective action to leading order in the hybridization and \mathbb{Z}_2 bond variables. The corresponding statistical mechanical model for the finite temperature behavior is a \mathbb{Z}_2 gauged spinor model,

$$H_{SU(2)} = -J \sum_{\langle i,j \rangle} \left[V_i^\dagger u_{ij} V_j + \text{H.c.} \right] - K \sum_q \prod_{\partial P_q} \hat{u}_{ij}. \quad (29)$$

In the presence of magnetic anisotropy or a Zeeman splitting, we can replace V_j by an x-y order parameter, $V_j \rightarrow e^{i\theta_j}$, so that this model reduces to the 3D \mathbb{Z}_2 -gauged XY model (or its 2+1 dimensional quantum equivalent) [30–32], where a lattice of XY rotors is gauged by \mathbb{Z}_2 field (Fig 5). The Hamiltonian for the \mathbb{Z}_2 gauged XY model is given by:

$$H_{qXY} = -J \sum_{\langle ij \rangle} u_{ij} \cos(\theta_i - \theta_j) - K \sum_q \prod_{\partial P_q} \hat{u}_{ij} \quad (30)$$

Here, each site has an XY order parameter parameterized by θ_i , and the bonds have a \mathbb{Z}_2 gauge field \hat{u}_{ij} on them (Fig. 5a), which multiplies the matter field θ_i s. Each flux plaquette P_q (“vison”) at q (Fig. 5a), costs an

energy $2K$ in the 3D cubic lattice. At small J , this model undergoes a pure gauge transition at a finite critical K_c in which the visons become linearly confined.

A more nuanced analysis of the 3D gauged XY model (30) is necessitated to understand the Higgs phase of the model. The J-K phase diagram of this model is understood in the various limits $J = 0$, $K = 0$, $K = \infty$ and $J = \infty$. At $J = 0$, there is a deconfinement transition at a finite $K = K_c$ into a phase where visons become linearly confined. At $K = 0$ there is an x-y phase transition into a phase where $\Psi_{2e} = e^{2i\theta}$ develops long range order, whilst at $K = \infty$, where the \mathbb{Z}_2 degrees of freedom are quenched, there is an x-y transition into a phase where $e^{i\theta}$ develops long range order. Finally at $J = \infty$, the ground-state manifold where $\cos(\theta_i - \theta_j) = u_{ij}$, is identical to that of the \mathbb{Z}_2 gauged Ising model considered by Fradkin and Shenkar [33], which has no phase boundary.

What is not known about the \mathbb{Z}_2 gauged Ising model, is whether the Ising deconfinement transition continues into the ordered phase. If the continuation is present, then there would be a vison-confining phase transition between a charge $2e$ and charge $1e$ order parameter. The phase boundary of this transition would have to continue to one of the corners of the phase diagram, that is to $J = \infty$ and either $K = 0$ or $K = \infty$ (see Fig 5b).

In drawing our tentative phase diagram of the CPT model, we have assumed that no such phase boundary exists. However, if it does, then the Ising transition, T_{c1} would extend inside the superconducting phase, corresponding to a transition from a charge- e fractionalized or-

dered phase to a charge- $2e$ composite ordered phase [22]. Future numerical analysis is required to confirm the existence of this transition.

One of the intriguing features of the proposed phase diagram (Fig. 2) are the two routes into the order-fractionalized phase: one originating from an FL* phase intertwined with a decoupled spin liquid, the other emerging directly from a heavy Fermi liquid. These two routes are reminiscent of the Bose-Einstein and BCS condensation pathways to a conventional superconductor. This raises the fascinating possibility that spinor superconducting order might develop as a novel superconducting instability of a Landau Fermi liquid. Unlike conventional triplet order, the fractionalized spinor order exhibits Kramer's degeneracy and a spontaneous broken time-reversal symmetry, even in situations where there are no conventional two-dimensional triplet representations, such as the orthorhombic triplet superconductor UTe₂. At present, the issue of whether UTe₂ spontaneously breaks time-reversal symmetry is a controversial point. Were the ground-state of this novel material to support broken time-reversal symmetry via a single sharp phase transition, this would constitute evidence for a fractionalized superconducting order parameter.

ACKNOWLEDGMENTS

Acknowledgments: This work was supported by Office of Basic Energy Sciences, Material Sciences and Engineering Division, U.S. Department of Energy (DOE) under Contracts No. DE-SC0012704 (AMT) and DE-FG02-99ER45790 (AP and PC).

Appendix A: Vison gap energy and Ising phase transition

In the CPT model [3, 4], the bond variables \hat{u}_{ij} commute with Kondo interaction and remain constants of motion. Consequently, the gauge fluctuations in the CPT model are thermal. Thermal gauge fluctuations in the hyper-octagonal Yao Lee spin liquid subside below the Ising critical temperature $T_{c,Ising}$. Free majoranas are the low-energy excitations in this regime.

In the order-fractionalized phase, the condensation of electron majorana pairs gaps out the majorana spectrum and Higgses the \mathbb{Z}_2 and Maxwell fields. This impacts the vison gap energy Δ_v , (the energy cost of one bond flip) in the fractionalized ordered phase. Given that the vison gap energy is the characteristic energy of \mathbb{Z}_2 gauge, the Ising critical temperature varies as the vison gap energy $T_{c1} \sim \Delta_v$. Indeed, Monte-Carlo simulations [21, 25] show that in 3D Kitaev spin liquids, the Ising critical temperature $T_{c,Ising}$, and the vison gap energy Δ_v are linearly correlated. Thus estimating vison gap energy Δ_v provides an estimate for the Ising critical temperature.

1. Vison gap energy of CPT Model

One can analytically determine the vison gap energy for Kitaev-like spin-liquids [34] by evaluating the change in free energy associated with flipping a local \mathbb{Z}_2 variable \hat{u}_{ij} (Fig. 6) away from the ground state gauge configuration. A flip in the local \mathbb{Z}_2 variable \hat{u}_{ij} acts as an impurity potential, leading to a scattering phase shift due to the Majoranas and a change in free energy, i.e., the vison gap energy Δ_v . This approach is validated against vison gap energy values obtained via Monte Carlo simulations, particularly for the $V = 0$ limit. For the isotropic case $J_x = J_y = J_z = K$, Monte Carlo simulations yield a vison gap energy of $\Delta_v = 0.09(1)K$ [21] for the Kitaev spin liquid on a hyperoctagon lattice (i.e. (10,3)a system). Our calculation aligns precisely with this result, yielding a vison gap energy of $\Delta_v = 0.089(5)K$ per Majorana species χ^a i.e. the Yao-Lee equivalent of Kitaev spin liquid. This methodology remains robust even when

the Majoranas hybridize with electrons, allowing us to extend the approach to the CPT model.

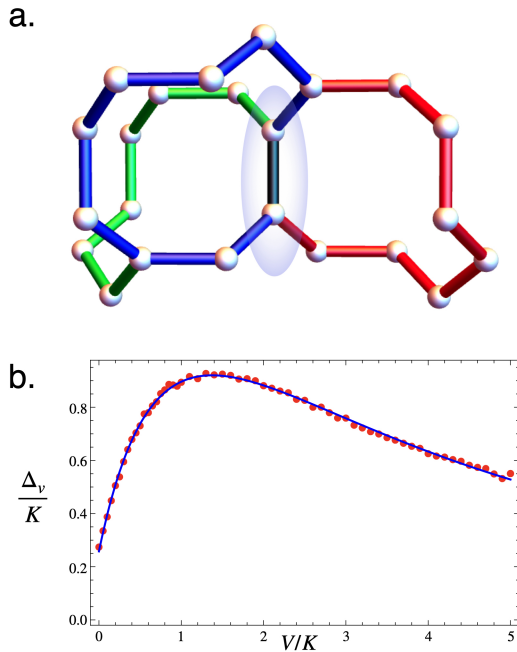


FIG. 6. (a) Shows the plaquettes in hyperoctagon lattice that change signs when one flips a bond variable $\hat{u}_{ij} = 1 \rightarrow -1$ shown in the oval, the energy. The energy cost associated with this flip is the vison gap energy (b)Vison gap energy as a function of hybridization calculated numerically on a $50 \times 50 \times 50$ unit cell lattice, with a hybridization resolution of $\frac{\Delta V}{K} = 0.01$. Consequently, we find the best fit for the vison gap energy as a function of hybridization V .

To compute the vison gap energy in the CPT model, we flip the \hat{u}_{ij} bond between the 2^{nd} and 3^{rd} atoms in the unit cell positioned at the origin,

$$H_{CPT+3v} = H_{CPT} - 2K(i\vec{\chi}_{0,2} \cdot \vec{\chi}_{0,3}). \quad (\text{A1})$$

H_{CPT+3v} is the Hamiltonian that has a local \mathbb{Z}_2 bond flip over this ground-state gauge configuration. This bond flip is associated with the creation of 3 visons adjacent to the bond. Treating the bond-flip term as an impurity potential,

$$\hat{V}_{flip} = -2K(i\vec{\chi}_{0,2} \cdot \vec{\chi}_{0,3}) \quad (\text{A2})$$

allows us to calculate the associated free-energy change. The free energy of the CPT model with \mathbb{Z}_2 bond flip is expressed in terms of its bare-Green's function $G_{0,CPT}$,

$$\beta F = -\frac{1}{2} \text{Tr} \log[-G_{0,CPT}^{-1} + \hat{V}_{flip}] \quad (\text{A3})$$

where $G_{0,CPT}(\omega, \vec{k}) = (\omega \mathbb{I} - h_{CPT}(\vec{k}))^{-1}$ is the Green's function for the CPT Model in the mean-field configuration.

Since the bond-flip potential \hat{V}_{flip} scatters Majorana fermions in the Yao-Lee spin liquid. The associated free-energy change is obtained in terms of effective majorana green's function $G_{\vec{\chi}}$, which includes self-energy corrections from the electron-majorana condensate, as follows

$$\Delta F = \frac{1}{2\beta} \text{Tr} \log[1 - \hat{V}_{flip} G_{\vec{\chi}}]. \quad (\text{A4})$$

Here, the trace is over the system and Matsubara frequencies.

The effective Majorana Green's function in the Majorana-electron condensate is given by,

$$G_{\vec{\chi}}(z, \vec{k}, V) = \frac{1}{z - Kh(\vec{k}) - \frac{V^2}{z + th(\vec{k})}} \quad (\text{A5})$$

Where V is the magnitude of the spinor order, and $h(\vec{k})$ is the 4-band Hamiltonian given in equation (8). This effective Green's function is used to calculate vison gap energy Δ_v by calculating the scattering phase shift of the \mathbb{Z}_2 bond-flip potential.

The scattering potential \hat{V}_{flip} is local, the free-energy of \mathbb{Z}_2 bond flip potential can be re-expressed in terms of the local majorana Green's function $g_{\vec{\chi}}(i\omega_n)$

$$\Delta F = \frac{1}{2\beta} \sum_{i\omega_n} [\ln(1 - \hat{V}_{flip} g_{\vec{\chi}}(i\omega_n))] \quad (\text{A6})$$

where, the local majorana Green's function $g_{\vec{\chi}}(i\omega_n)$ is,

$$g_{\vec{\chi}}(z) = \frac{1}{N_c} \sum_{k \in BZ} G_{\vec{\chi}}(z, k) \quad (\text{A7})$$

obtained by summing the Majorana Green's function over the Brillouin zone. Upon carrying out the Matsubara frequency summation, one obtains the expression of the free-energy change in terms of the scattering phase shift,

$$\Delta F = \int_{-\infty}^{\infty} \frac{d\omega}{2\pi} \left(\frac{1}{2} - f(\omega) \right) \delta_v(\omega) \quad (\text{A8})$$

where, the scattering phase shift δ_v is given by

$$\delta_v(\omega) = \text{Im} \text{Tr} \log[1 - \hat{V}_{flip} g_{\vec{\chi}}(z)]_{z=\omega-i\delta}. \quad (\text{A9})$$

At zero-temperature, this free-energy change corresponds to the vison gap energy Δ_v given by,

$$\Delta_v = -K \int_{-\infty}^0 \frac{dx}{2\pi} \text{Im} \log[\det(1 - \hat{V}_{flip} g_{\vec{\chi}}(z))]_{z=x-i\delta}. \quad (\text{A10})$$

Where the Tr is over the sites within the unit-cells. Numerically, the vison gap energy calculation was carried out on a $50 \times 50 \times 50$ lattice by carrying out discrete summation over the momentum in the Brillouin zone and frequencies.

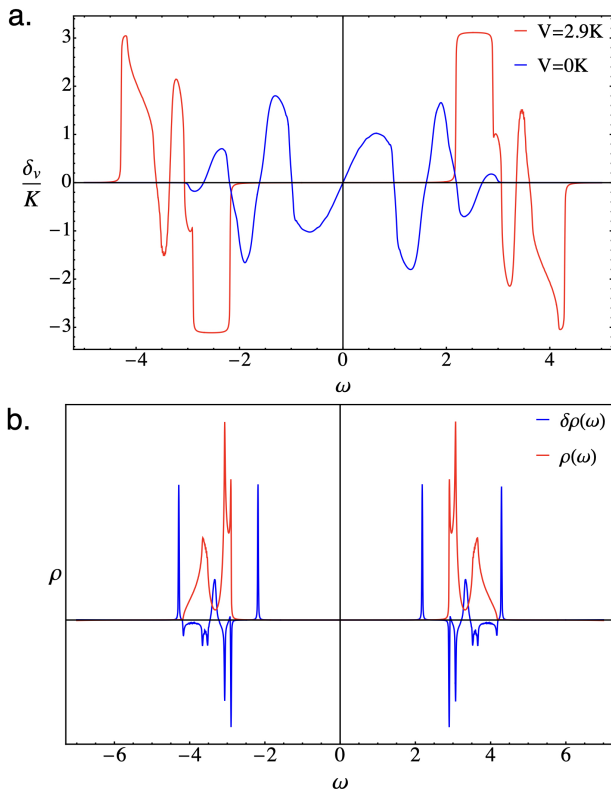


FIG. 7. (a) Depicts the scattering phase shift associated with a bond flip impurity \hat{V}_{flip} for a species of spin Majorana χ^a , illustrating two spinor order strengths: $V = 0K$ (in blue) and $V = 2.9K$ (in red). The plateau for the gapped $V = 2.9K$ state at $\Delta_v = \pi$ signifies the formation of an in-gap bound state. (b) Shows the change in density of states $\delta\rho = \frac{1}{2\pi} \frac{d\delta_v(\omega)}{d\omega}$ (in blue) associated with the bond flip potential \hat{V}_{flip} . The sharp peak inside the gap (shown using the bulk density of state ρ for $V = 2.9K$ in red) signifies the presence of an in-gap bound state for spinor order strength of $V = 2.9K$.

We compute the vison gap energy for discrete values of hybridization V with a resolution of $\frac{\Delta V}{t} = 0.01$. The resulting dataset was fit to obtain a functional form,

$$\Delta_v(V) = r \left(\frac{1}{(sV + u)^2} - \frac{1}{(sV + u)^4} \right) \quad (\text{A11})$$

with $s = 0.273$, $u = 1.040$ and $r = 3.680$. This function form matches the asymptotic behavior of the vison gap energy $\Delta_v \sim \frac{1}{\sqrt{z}}$ for large V , which is always positive and is obtained analytically using equation (A10). Additionally, it also matches the numerical result [21] for $V = 0$ as can be seen in (Fig. 6), and consequently is a reliable fit. The initial enhancement in the vison gap energy Δ_v is a consequence of \mathbb{Z}_2 gauge theories being Higgs phases of continuum gauge theories [32, 35], thus electron-majorana fractionalized order formation enhances the already massive \mathbb{Z}_2 gauge fields. The reduction in the vison gap energy Δ_v for large hybridization Δ_v is a result of renormalization effects at large Kondo coupling J .

Since the vison gap energy in the CPT model asymptotically decreases as $\Delta_v \sim \frac{1}{\sqrt{z}}$ for large hybridization V . Thus, as the Kondo coupling J increases, the characteristic vison gap energy scale renormalizes to smaller values as a result of Kondo screening. Additionally, given the linear correlation between vison-gap energy and Ising critical temperature $T_{c,Ising}$, we estimate that Ising critical temperature $T_{c,Ising} \sim \Delta_v \sim \frac{1}{\sqrt{z}}$ reduces with increasing Kondo coupling. Beyond this Ising critical temperature scale $T_{c,Ising}$, the thermal gauge fluctuations destroy electron-majorana fractionalized order.

The electron-majorana fractionalized order in the CPT model is expected to be suppressed by quantum fluctuations about the mean-field theory. Such quantum fluctuations will grow as one moves away from the small Kondo coupling J regime, where the J is the small parameter that controlling the mean-field treatment. In the large Kondo coupling J limit, the ground state is a Kondo insulator with a decoupled orbital Kitaev spin liquid. Thus, passing from the superconducting electron-majorana condensate at small J to the Kondo insulator phase at large J , the system undergoes a quantum phase transition. Away from half-filling, this quantum phase transition is associated with the small-to-large expansion of the neutral Fermi surface, a likely signature of a continuous quantum phase transition.

-
- [1] C. Petrovic, P. G. Pagliuso, M. F. Hundley, R. Movshovich, J. L. Sarrao, J. D. Thompson, Z. Fisk, and P. Monthoux, *Journal of Physics: Condensed Matter* **13**, L337 (2001).
- [2] R. Flint, M. Dzero, and P. Coleman, *Nature Physics* **4**, 643 (2008).
- [3] A. M. Tsvelik and P. Coleman, *Physical Review B* **106**, 125144 (2022).
- [4] P. Coleman, A. Panigrahi, and A. Tsvelik, *Physical Review Letters* **129**, 177601 (2022).
- [5] W. Choi, P. W. Klein, A. Rosch, and Y. B. Kim, *Physical Review B* **98**, 155123 (2018).
- [6] U. F. P. Seifert, T. Meng, and M. Vojta, *Physical Review B* **97**, 085118 (2018).
- [7] M. Dzero, K. Sun, V. Galitski, and P. Coleman, *Physical Review Letters* **104**, 106408 (2010).
- [8] M. Neupane, N. Alidoust, S.-Y. Xu, T. Kondo, Y. Ishida, D. J. Kim, C. Liu, I. Belopolski, Y. J. Jo, T.-R. Chang, H.-T. Jeng, T. Durakiewicz, L. Balicas, H. Lin, A. Bansil, S. Shin, Z. Fisk, and M. Z. Hasan, *Nature Communications* **4**, 2991 (2013).
- [9] Z.-D. Song and B. A. Bernevig, *Physical Review Letters*

- 129, 047601 (2022).**
- [10] A. Kumar, N. C. Hu, A. H. MacDonald, and A. C. Potter, *Physical Review B* **106**, L041116 (2022).
- [11] A. Ramires and J. L. Lado, *Physical Review Letters* **121**, 146801 (2018).
- [12] P. Coleman, *Physical Review B* **28**, 5255 (1983).
- [13] N. Read and D. M. Newns, *Journal of Physics C: Solid State Physics* **16**, 3273 (1983).
- [14] J. B. Kogut, *Reviews of Modern Physics* **51**, 659 (1979).
- [15] T. Senthil, M. Vojta, and S. Sachdev, *Phys. Rev. Lett* **90**, 216403 (2003).
- [16] P. Coleman, J. B. Marston, and A. J. Schofield, *Phys. Rev. B* **72**, 245111. 15 p (2005).
- [17] A. Kitaev, *Annals of Physics* **321**, 2 (2006).
- [18] H. Yao and D.-H. Lee, *Physical Review Letters* **107**, 087205 (2011).
- [19] M. Hermanns and S. Trebst, *Phys. Rev. B* **89**, 235102 (2014).
- [20] M. Hermanns, I. Kimchi, and J. Knolle, *Annual Review of Condensed Matter Physics* **9**, 17 (2018).
- [21] K. O'Brien, M. Hermanns, and S. Trebst, *Physical Review B* **93**, 085101 (2016).
- [22] Y. Komijani, A. Toth, P. Chandra, and P. Coleman, (2018), 10.48550/ARXIV.1811.11115, publisher: arXiv Version Number: 2.
- [23] U. F. P. Seifert, X.-Y. Dong, S. Chulliparambil, M. Vojta, H.-H. Tu, and L. Janssen, *Phys. Rev. Lett.* **125**, 257202 (2020).
- [24] P. A. Mishchenko, Y. Kato, and Y. Motome, *Phys. Rev. B* **96**, 125124 (2017).
- [25] T. Eschmann, P. A. Mishchenko, K. O'Brien, T. A. Bojesen, Y. Kato, M. Hermanns, Y. Motome, and S. Trebst, *Physical Review B* **102**, 075125 (2020).
- [26] M. Hermanns, S. Trebst, and A. Rosch, *Phys. Rev. Lett.* **115**, 177205 (2015).
- [27] P. Coleman, C. Pépin, Q. Si, and R. Ramazashvili, *Journal of Physics: Condensed Matter* **13**, R723 (2001).
- [28] T. Senthil, M. Vojta, and S. Sachdev, *Physical Review B* **69**, 035111 (2004).
- [29] S. Paschen, T. Lühmann, S. Wirth, P. Gegenwart, O. Trovarelli, C. Geibel, F. Steglich, P. Coleman, and Q. Si, *Nature* **432**, 881 (2004).
- [30] P. E. Lammert, D. S. Rokhsar, and J. Toner, *Physical Review Letters* **70**, 1650 (1993).
- [31] P. E. Lammert, D. S. Rokhsar, and J. Toner, *Physical Review E* **52**, 1778 (1995).
- [32] S. Sachdev, *Reports on Progress in Physics* **82**, 014001 (2019).
- [33] E. Fradkin and S. H. Shenker, *Physical Review D* **19**, 3682 (1979).
- [34] A. Panigrahi, P. Coleman, and A. Tsvelik, *Physical Review B* **108**, 045151 (2023).
- [35] E. Fradkin, *Quantum field theory: an integrated approach* (Princeton University Press, Princeton, 2021).